

Precision ESR Measurements of Transverse Anisotropy in the Single-molecule Magnet Ni_4

Charles A. Collett,¹ Rafael A. Allão Cassaro,² and Jonathan R. Friedman¹

¹*Department of Physics and Astronomy, Amherst College, Amherst 01002, USA*

²*Instituto de Química, Universidade Federal do Rio de Janeiro, Rio de Janeiro, RJ, 21945-970 Brazil*

(Dated: October 3, 2016)

We present a method for precisely measuring the tunnel splitting in single-molecule magnets (SMMs) using electron-spin resonance, and use these measurements to precisely and independently determine the underlying transverse anisotropy parameters, given a certain class of transitions. By diluting samples of the SMM Ni_4 via co-crystallization in a diamagnetic isostructural analogue we obtain markedly narrower resonance peaks than are observed in undiluted samples. Using custom loop-gap resonators we measure the transitions at several frequencies, allowing a precise determination of the tunnel splitting. Because the transition under investigation occurs at zero field, and arises due to a first-order perturbation from the transverse anisotropy, we can determine the magnitude of this anisotropy independent of any other Hamiltonian parameters. This method can be applied to other SMMs with tunnel splittings arising from first-order transverse anisotropy perturbations.

Single-molecule magnets (SMMs) have the potential to be used as spin qubits, combining the simplicity of a single large-spin system with the tunability afforded by chemical engineering. One of the main challenges for the use of such systems is that the proximity of the molecules within a crystal causes significant dipolar interactions, leading to decoherence of the quantum spin state. One method for reducing dipolar interactions in molecular spin systems is applying high fields to polarize the system; this method was used to show the importance of such interactions in decoherence.^{1,2} Another approach is to dilute the sample, spacing the magnetic molecules apart within a diamagnetic environment either by dissolving samples in an appropriate solvent^{3,4} or by co-crystallizing molecules with diamagnetic analogues.^{5,6} The co-crystallization technique has the advantage that the system is crystalline and the molecules therefore retain orientational order. In addition, recent experiments have focused on atomic-clock transitions as another method of minimizing decoherence: by working at an avoided level crossing, the decoherence time T_2 can be significantly enhanced.⁶⁻⁸ In this work, we present a method for using electron-spin resonance (ESR) to precisely measure the zero-field tunnel splitting in SMMs with splittings of order $\Delta/h = f \approx 1 - 10$ GHz. By combining dilution via co-crystallization with custom-designed resonators and a tunnel splitting that is determined through first-order perturbation theory, this method allows the determination of the transverse anisotropy independently from any other Hamiltonian parameters. This precise determination of the tunnel splitting permits experiments to be tuned precisely to the clock transition, maximizing spin coherence.

Here we consider the SMM $[\text{Ni}(\text{hmp})(\text{dmb})\text{Cl}]_4$ (“ Ni_4 ”), a system with spin $S = 4$,⁹ where hmp stands for 2-hydroxymethylpyridine and dmb for 3,3-dimethyl-1-butanol. Based on this molecule’s four-fold symmetry,

it can be described by the “giant spin” Hamiltonian

$$\mathcal{H} = -DS_z^2 - AS_z^4 + C(S_+^4 + S_-^4) + \mu_B \vec{B} \cdot \mathbf{g} \cdot \vec{S}, \quad (1)$$

where D and A are axial anisotropy parameters, C is the transverse anisotropy parameter, \mathbf{g} is the g-tensor, and \vec{B} is the applied magnetic field. This Hamiltonian describes a system with an easy axis (z). The transverse anisotropy term breaks the symmetry of the molecule and permits tunneling between levels with $\Delta m = \pm 4n$ (integer n). Determining the exact energy spectrum for such an SMM is normally accomplished by performing high-frequency ESR at various magnetic fields and fitting the resonance peaks to energies described by the Hamiltonian.^{10,11} This approach yields values of all relevant Hamiltonian parameters, but is less sensitive to the transverse anisotropy terms, as they are generally significantly smaller than the axial anisotropy terms, meaning that the transverse terms can typically only be determined to about one digit of precision.

More direct measurements of the transverse anisotropy can be done, such as the experiment by Shiddiq *et al.*⁶ They studied the SMM HoW_{10} , diluted by co-crystallization, and measured the splitting $\Delta_{\pm 4}$ between $m = \pm 4$ spin states, which is connected by the $C(S_+^4 + S_-^4)$ transverse anisotropy. In that case, where $\Delta m = 8$, the states are coupled through second-order perturbation theory, meaning that the splitting depends on both C and D : $\Delta_{\pm 4} \propto C^2/|D|$. By performing a similar experiment on the Ni_4 system using states connected through a first-order perturbation, we are able to directly measure C for this system with no reliance on other Hamiltonian parameters.

We studied Ni_4 diluted by co-crystallization with Zn_4 , an isostructural diamagnetic molecule. This dilution leaves the majority of the Ni_4 molecules intact and allows control of the average intermolecular distance between Ni_4 centers. Details on this synthesis will be presented elsewhere.¹² Ni_4 can be well described by Eq. 1, and has a significant transverse anisotropy term C , which produces

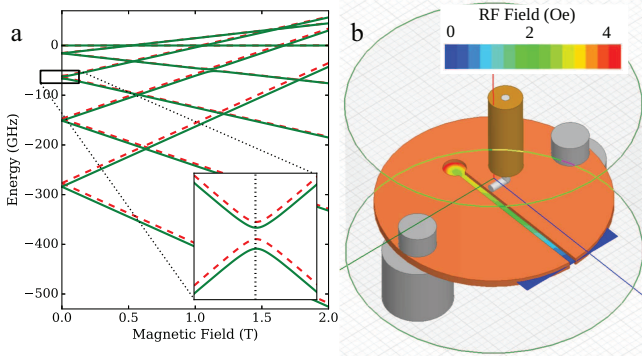


FIG. 1. (a) Energy-level diagram for Ni_4 as a function of field along the z axis. Inset: Zoomed-in view of the avoided crossing for the $|\pm 2\rangle$ states near zero field for both conformational states. Solid green and red dashed lines show the levels corresponding to the two different conformational states of the molecule. (b) Schematic of LGR inside a copper shield, with excitations provided by an antenna. The color map in the central loop and gap shows the magnitude of the rf magnetic field for a given excitation amplitude, yielding a strong uniform field in the center of the loop. Produced using ANSYS Electromagnetics Suite, Release 16.2.

a tunnel splitting of $\Delta_{\pm 2} \sim 4$ GHz between the $m = \pm 2$ states at zero field. Figure 1(a) shows the energy-level diagram for Ni_4 , with the inset highlighting this splitting. At low temperatures, Ni_4 undergoes a transition into two distinct ligand conformational states, each of which have slightly different energies as shown by the green solid and red dashed lines in Fig. 1(a), leading to a doubling of the ESR spectra.^{11,13} The effects of this conformational change on the spin Hamiltonian are not fully understood, allowing the possibility that the four-fold symmetry of Ni_4 is broken, which could introduce a second-order transverse anisotropy term. In the absence of evidence for such symmetry-breaking, or higher-order transverse anisotropy terms such as $S_z^2 (S_+^4 + S_-^4) + h.c.$, we assume that the only significant contribution to the splitting is the fourth-order “ C term”.

For small fields applied along the easy axis, the field dependence of the splitting of the levels shown in the inset to Fig. 1(a) can be well described by

$$f_{\pm 2} = \sqrt{\Delta_{\pm 2}^2 + (g_z \mu_B (m - m') B)^2}, \quad (2)$$

where $\Delta_{\pm 2}$ is the zero-field splitting, m and m' are the quantum numbers associated with the levels far from the avoided crossing — 2 and -2, respectively, for the case studied here — and g_z is the g factor along the z axis. All energies are measured in units of frequency.

ESR measurements were done by placing single-crystal samples of Ni_4 in the loop of a loop-gap resonator (LGR)¹⁴ designed to match specific frequencies. LGRs produce a uniform high rf magnetic field in the loop, as shown schematically in Fig. 1(b). The dimensions of the loop are small compared with the wavelength, allowing a high filling factor to be achieved. Our LGRs typ-

ically have quality factors of $Q \sim 2000$. Their resonant frequency can also be tuned by introducing a dielectric such as sapphire into the gap, giving the resonators used in this work an effective range of several hundred MHz. By sweeping the field, we move the sample on and off resonance with the LGR, producing dips in Q when the sample couples to the resonator. The samples studied here were aligned to minimize θ , the angle between the easy axis and the DC field, such that $\theta < 10^\circ$, making Eq. 2 a valid description of the splitting.

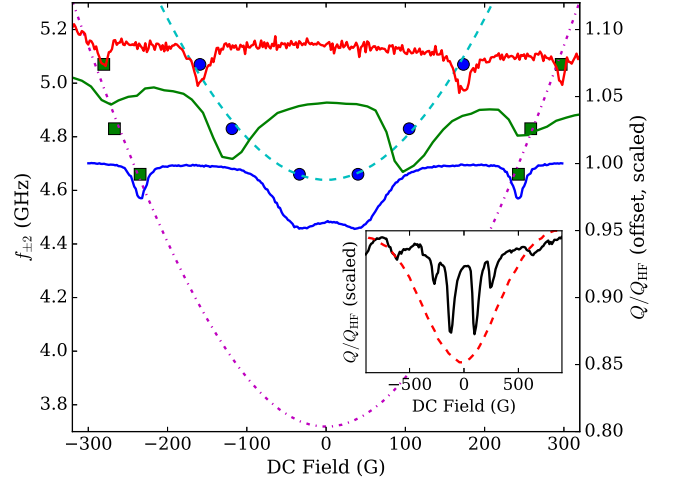


FIG. 2. ESR spectra (right axis, Q/Q_{HF} vs. H) for 4.655 (blue, lowest), 4.833 (green, middle), and 5.072 GHz (red, highest) at 10 K, offset by their frequency difference and scaled for clarity, where Q_{HF} is the high-field value of Q for each trace. Transitions appear as dips in Q/Q_{HF} . Blue circles and green squares show the frequency (left axis) and field locations of the transitions, from Lorentzian fits to the dips. The dashed blue and dash-dotted purple lines show fits to these data to Eq. 2, resulting in tunnel splittings of $\Delta_{\pm 2,1} = 4.64(2)$ GHz and $\Delta_{\pm 2,2} = 3.72(20)$ GHz. Inset: Scaled spectra at 4.8 GHz and 10 K for 100% Ni_4 (red dashed line) and dilute $(\text{Ni}_4)_{0.05}(\text{Zn}_4)_{0.95}$ (black solid line). The peaks at $\sim \pm 600$ G in the dilute spectrum arise from impurities in the apparatus and are not associated with the sample.

Figure 2 shows $(\text{Ni}_4)_{0.05}(\text{Zn}_4)_{0.95}$ (5% dilute Ni_4) spectra taken at $\nu = 4.655, 4.833$, and 5.072 GHz, showing peaks (symmetric around zero field) associated with transitions between the states shown in the inset of Fig. 1; the peaks at lower (higher) fields correspond to transitions associated with the green solid (red dashed) levels. For comparison purposes, the inset shows spectra at $\nu = 4.8$ GHz for 100% Ni_4 (red dashed line) and 5% dilute Ni_4 (black solid line), illustrating the effectiveness of dilution in enabling the resolution of the fine features we are investigating (the four central peaks). The precision of our experiment relies on being able to resolve these fine features. By fitting the spectral peaks for the dilute $(\text{Ni}_4)_{0.05}(\text{Zn}_4)_{0.95}$ sample to Lorentzian functions, we extracted the field location for each peak at each frequency. Figure 2 shows the observed frequency-field relation for

peaks from each conformational state as blue circles and green squares. We fit this data to Eq. 2; in order to determine $\Delta_{\pm 2}$, no assumptions need be made about g_z as $\Delta_{\pm 2}$ is independent of B . We applied this fitting for both conformational states, and the resulting fits are shown as the blue dashed line and the purple dash-dotted line in Fig. 2, yielding splitting values of $\Delta_{\pm 2,1} = 4.64(2)$ GHz and $\Delta_{\pm 2,2} = 3.72(20)$ GHz. Using first-order perturbation theory, one can show that this splitting is related to the transverse anisotropy through $\Delta_{\pm 2} = 720C$, which gives $C_1 = 6.44(3)$ MHz and $C_2 = 5.16(27)$ MHz for the two conformational states. These values are in reasonably good agreement with previous measurements^{15,16} of $C = 6$ MHz, but give much greater precision and allow us to differentiate the values associated with the two conformational states. The uncertainty in the determination of the splitting for the second state is significantly higher than the first, due to the lack of data near its zero-field frequency. From the fit to Eq. 2, we can also extract g_z values of $g_{z,1} = 2.18(8)$ and $g_{z,2} = 2.11(16)$, which are consistent with each other and with values determined at much higher fields.¹³

Our work gives precise measurements of the transverse anisotropy parameter C , independent of the value of any other spin Hamiltonian parameters. Given the symmetry of the molecule (S_4 in this case), we attribute the splitting to arise from the transverse C term in Eq. 1, which is the leading-order term consistent with the symmetry. Without measurements of other tunnel splittings, we cannot rule out contributions from higher-order transverse anisotropy terms in the Hamiltonian. Neglecting the small effect of such possible terms, we can relate the

splitting of the observed transition to C through first-order perturbation theory. Since our experiment involves applying the field along the easy axis of the system, we do not gain information about the direction of the hard axes (x and y) relative to the crystallographic directions. A careful study of the behavior of the tunnel splitting on the azimuthal direction of a field applied in the x - y plane should allow a precise determination of the hard-axis directions. In fact, when the field is applied along a hard axis, a geometric-phase-interference effect should cause the tunnel splitting to be suppressed for certain field magnitudes.^{17–19} While the work herein considers systems with four-fold symmetry, a similar technique can be applied to SMMs with lower symmetry, where the dominant transverse anisotropy would have the form $\frac{E}{2}(S_+^2 + S_-^2)$ and the value of E could be determined directly by measuring the splitting between $m = \pm 1$ states at zero field.

ACKNOWLEDGMENTS

We thank C. Yoo for his work on the design and development of the resonators and J. Kubasek for assistance in fabrication of the resonators. Support for this work was provided by the U. S. National Science Foundation under Grant No. DMR-1310135 and by the Amherst College Dean of Faculty. R.A.A.C. acknowledges CAPES and CNPq for financial support. J.R.F. acknowledges the support of the Amherst College Senior Sabbatical Fellowship Program, funded in part by the H. Axel Schupf '57 Fund for Intellectual Life.

¹ S. Takahashi, J. van Tol, C. C. Beedle, D. N. Hendrickson, L.-C. Brunel, and M. S. Sherwin, *Physical Review Letters* **102**, 087603 (2009).

² S. Takahashi, I. S. Tupitsyn, J. van Tol, C. C. Beedle, D. N. Hendrickson, and P. C. E. Stamp, *Nature* **476**, 76 (2011).

³ A. Ardavan, O. Rival, J. J. L. Morton, S. J. Blundell, A. M. Tyryshkin, G. A. Timco, and R. E. P. Winpenny, *Phys. Rev. Lett.* **98**, 057201 (2007).

⁴ C. Schlegel, J. van Slageren, M. Manoli, E. K. Brechin, and M. Dressel, *Physical Review Letters* **101**, 147203 (2008).

⁵ J. J. Henderson, C. M. Ramsey, E. del Barco, T. C. Stamatatos, and G. Christou, *Physical Review B* **78**, 214413 (2008).

⁶ M. Shiddiq, D. Komijani, Y. Duan, A. Gaita-Ario, E. Coronado, and S. Hill, *Nature* **531**, 348 (2016).

⁷ D. Vion, A. Aassime, A. Cottet, P. Joyez, H. Pothier, C. Urbina, D. Esteve, and M. H. Devoret, *Science* **296**, 886 (2002).

⁸ G. Wolfowicz, A. M. Tyryshkin, R. E. George, H. Riemann, N. V. Abrosimov, P. Becker, H.-J. Pohl, M. L. W. Thewalt, S. A. Lyon, and J. J. L. Morton, *Nature Nanotechnology* **8**, 561 (2013).

⁹ E.-C. Yang, W. Wernsdorfer, L. N. Zakharov, Y. Karaki, A. Yamaguchi, R. M. Isidro, G.-D. Lu, S. A. Wilson,

A. L. Rheingold, H. Ishimoto, and D. N. Hendrickson, *Inorganic Chemistry* **45**, 529 (2006).

¹⁰ S. Ghosh, S. Datta, L. Friend, S. Cardona-Serra, A. Gaita-Ario, E. Coronado, and S. Hill, *Dalton Transactions* **41**, 13697 (2012).

¹¹ J. Lawrence, E.-C. Yang, R. Edwards, M. M. Olmstead, C. Ramsey, N. S. Dalal, P. K. Gantzel, S. Hill, and D. N. Hendrickson, *Inorganic Chemistry* **47**, 1965 (2008).

¹² C. A. Collett *et al.*, In Preparation (2016).

¹³ Y. Chen, M. D. Ashkezari, C. A. Collett, R. A. Allão Casaro, F. Troiani, P. M. Lahti, and J. R. Friedman, *Phys. Rev. Lett.*, accepted (2016), arxiv:1510.03109 [cond-mat].

¹⁴ G. A. Rinard and G. R. Eaton, *Biomedical EPR, Part B: Methodology, Instrumentation, and Dynamics*

¹⁵ C. Kirman, J. Lawrence, S. Hill, E.-C. Yang, and D. N. Hendrickson, *Journal of Applied Physics* **97**, 10M501 (2005).

¹⁶ G. de Loubens, D. A. Garanin, C. C. Beedle, D. N. Hendrickson, and A. D. Kent, *Europhysics Letters* **83**, 37006 (2008).

¹⁷ C.-S. Park and A. Garg, *Physical Review B* **65**, 064411 (2002).

¹⁸ G.-H. Kim, *Journal of Applied Physics* **91**, 3289 (2002).

¹⁹ S. T. Adams, E. H. da Silva Neto, S. Datta,

J. F. Ware, C. Lampropoulos, G. Christou, Y. Myaesoedov, E. Zeldov, and J. R. Friedman,
Physical Review Letters **110**, 087205 (2013).